# PARAMETRIC ANALYSIS OF ROOT LOCATION FOR A FOURTH-ORDER CHARACTERISTIC EQUATION

A. V. Sorokvashin* and A. I. Ignatov**

*,** Bauman Moscow State Technical University, Moscow, Russia

*✉ sorokvashinav@student.bmstu.ru, **✉ ignatov@bmstu.ru

**Abstract.** This paper develops a root-based method for analyzing dynamic systems with fourth-order characteristic equations based on a spatial analog of the Vyshnegradsky diagram. Such an approach allows visualizing system stability and, moreover, determining key performance indices of transients without directly computing the roots. Within the proposed methodology, a parametrization of complex surfaces is employed to construct a three-dimensional (3D) root location diagram for a fourth-order characteristic equation. On this diagram, the solutions are divided into stable and unstable ones by the stability boundary. The surface of zero discriminant is used to classify the roots into real and complex. An additional surface defines the boundary of different root locations relative to the imaginary axis. A method for deriving these parametrically defined surfaces is presented. Parametric expressions are obtained for families of surfaces corresponding to particular system performance requirements (level surfaces for the stability degree, the oscillatory index, and the maximum absolute value among the real parts of all roots). The research results can be conveniently applied in practice to design automatic control systems. The 3D diagrams constructed in MATLAB visualize the parameter regions simultaneously ensuring the desired values of transient characteristics, the response speed, and the oscillatory index.

**Keywords**: Vyshnegradsky stability diagram, fourth-order system, characteristic equation, stability, discriminant, root location, parametrization, oscillation.

## INTRODUCTION

The design of automatic control systems is invariably associated with ensuring the required quality of transients. Stability is the most important property of a system, and its settling time, oscillatory index, and overshoot are key performance criteria. When studying transients based on the linearization of differential equations, one formulates requirements for the dynamic properties of a system by imposing conditions on the roots of the corresponding characteristic equations. Stability and the above performance indices are related to the mutual arrangement of roots (root location) for a characteristic equation in the complex plane, which forms the foundation of root-based methods of performance assessment. This approach was applied and studied, e.g., in [1, 2].

To constrain a root location region (Fig. 1), the stability degree $\eta$, the oscillatory index $\mu$, and the absolute value $\xi$ of the real part of the characteristic equation root with the largest distance to the imaginary axis (the maximum absolute value among the real parts of all roots) are commonly used [3].

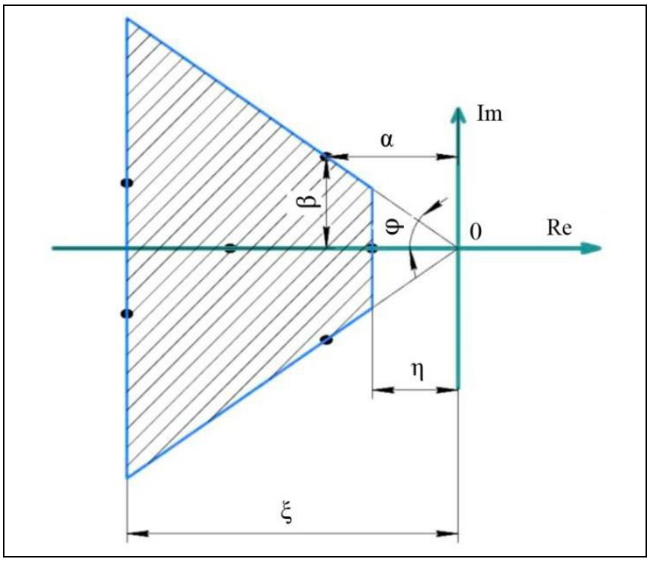


**Fig. 1. A root location region.**

The stability degree η is defined as the absolute value of the real part of the characteristic equation root with the smallest distance to the imaginary axis. This parameter is related to the system's response time:

$$T_{\text{set}} \approx \frac{1}{\eta}\ln\left(\frac{1}{\Delta}\right),$$

where $T_{\text{set}}$ is the settling time, and Δ is an admissible relative deviation of the controlled variable. Thus, increasing the stability degree of a system reduces its settling time.

The oscillatory index of a system is defined as the tangent of the angle formed by the negative real half-axis and the ray from the origin to the root with the maximum ratio of the imaginary and real parts:

$$\mu = \text{tg}\phi = \max\left(\frac{\beta}{\alpha}\right),$$

where α and β are the real and imaginary parts of the roots, respectively. The oscillatory index is related to the logarithmic decay rate:

$$d = \frac{2\pi}{\mu}.$$

In other words, the oscillatory index μ is proportional to the number of oscillations $1/d$ after which the amplitude of the oscillations decreases by a factor of $e$.

According to automatic control theory, overshoot is expressed via the oscillatory index as

$$\sigma_{\max} = e^{-\frac{\pi}{\mu}}.$$

Fourth-order systems cannot contain high-order controllers, and low-order controllers are described by a small set of parameters. Low-order controllers are preferred primarily because of their ease of tuning; however, it is often possible to achieve better performance results using relatively simple controllers and less complex design algorithms [4].

Graphical methods stand out as particularly advantageous for the design and analysis of dynamic systems. An important benefit of these methods is the ability to study the close neighborhood of a selected point: the system can be assessed if the actual parameter values deviate from nominal ones; and the engineer has some freedom of choice for system parameters within an admissible region. Of course, small changes in system parameters can sometimes significantly influence its performance; however, graphical methods usually mitigate such effects. In this context, we mention the classical D-decomposition (D-partition), as its modifications are still actively used in practice [4, 5]. In particular, the Kharitonov theorem was applied in [5] to stabilize a system with interval parametric uncertainty; according to this theorem, the stability of such a system is established based on the stability of a finite set of characteristic polynomials. And the region of admissible solutions was constrained, among other things, by admissible values of the oscillatory index and the stability degree [5]. As noted therein, Kharitonov polynomials can be used to ensure the required values of these parameters under interval uncertainty.

For third-order systems, the Vyshnegradsky diagram serves as a classical and intuitive analytical tool. Within this approach, the dynamic properties of the system are investigated by analyzing the Vyshnegradsky parameters $A$ and $B$ of the normalized characteristic equation

$$x^3 + Ax^2 + Bx + 1 = 0$$

without directly computing the roots. This approach [6] is easily implemented using modern tools (e.g., in MATLAB).

The Vyshnegradsky diagram (Fig. 2) represents a plane of the parameters $A$ and $B$, divided into regions corresponding to different natures of transients. The stability region is bounded by the coordinate axes and the hyperbola $AB = 1$. This region contains three characteristic subregions as follows: *I*, where the complex roots are located closer to the imaginary axis (an oscillatory process); *II*, where all roots are real (an aperiodic process); and *III*, where a real root is located closer to the imaginary axis (a monotonic process).

To pass from the analysis to design of systems satisfying specified requirements for the response time and the oscillatory index, the Vyshnegradsky diagram is supplemented with grids of level lines for η, μ, and ξ. In practice, the region of admissible system parameters is narrowed to the intersection of zones bounded by the lines of the required stability degree and admissible values of the oscillatory index. As a result, one chooses controller parameters simultaneously ensuring the desired response speed and damping nature. An example of this approach was provided in [7].

The most successful conceptual extension of the Vyshnegradsky diagram was described in the monograph [8]. The authors used parameters different from those of Vyshnegradsky to derive some exact and approximate algebraic conditions for obtaining the desired values of the system's performance indices; also, they generalized the original approach to systems

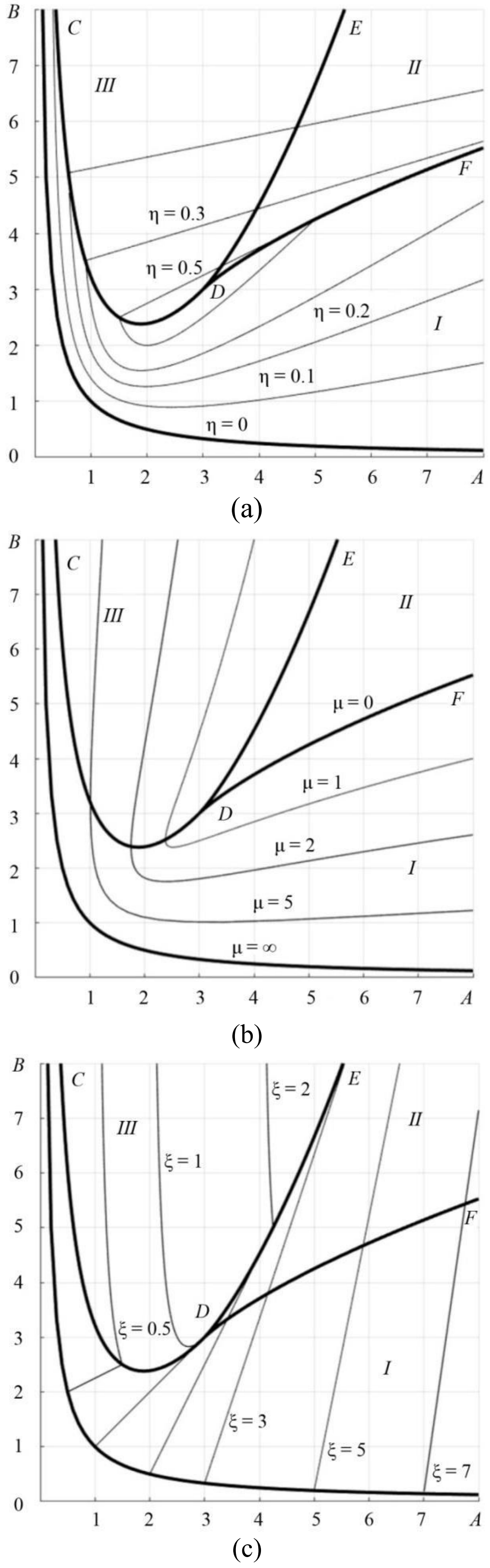


**Fig. 2. The Vyshnegradsky diagram with level lines for** (a) the stability degree, (b) the maximum absolute value among the real parts of all roots, and (c) the oscillatory index.

of any order. The authors' graphical relationships (quality nomograms) for determining several transient performance indices (rise time, overshoot, the oscillatory index, passband, and cutoff frequency) of fourth-order and higher-order systems were constructed primarily using numerical methods and approximations. Therefore, it is difficult to derive the nomograms directly compared to approaches involving only analytical relationships. A combined three-dimensional (3D) quality nomogram in the form of a series of 2D cross-sections, as well as a 2D universal quality nomogram, were proposed. Direct application of a series of 2D nomograms from the monograph does not seem convenient under current conditions, although the idea of "digitizing" such nomograms appears quite promising.

In this paper, we develop Vyshnegradsky's approach and construct its direct analog for fourth-order systems. This is of considerable practical interest for the design of more complex dynamic systems. Note that solution and analysis methods for fourth-order systems are still being studied and systematized [9]. For example, a detailed classification of fourth-order equations based on the number and multiplicity of their real roots was provided in [10]. The features of equations with multiple roots were primarily considered in [11], although some of the conclusions can be extended to fourth-order equations without multiple roots. Matrix methods are also widely used for fourth-order systems, e.g., the technique of linear matrix inequalities (LMIs) [12]. With this technique, one obtains the system parameters localizing the roots within a given region of the complex plane. The Ackermann formula, as well as its generalizations [13] and simplifications [14], localizes the roots to a predefined region. Standard polynomials (Newton, Butterworth, Bessel, and others) are often taken as such suitable root locations [15], although (generally speaking) it is impossible to obtain a characteristic equation in the form of a standard polynomial while considering all system requirements and constraints imposed on the coefficients.

Some attempts to reinterpret the Vyshnegradsky diagram, including an extension to the fourth order, were made in [16] and [17]. In particular, the surface of zero discriminant was constructed and studied in [17]. This surface, as well as the nature of the roots in the regions separated by it, was considered in [18] and [19]. Discriminants and their relationship to the multiplicity of roots were discussed in detail in [20]. An in-depth study of the roots of a fourth-order equation, including the construction of a series of diagrams, was undertaken in [21].

The main assumption accepted below is that a system is described by a linear time-invariant model, and its dynamic properties are entirely determined by the root location for the corresponding fourth-order characteristic equation. Also, we suppose that the performance requirements for transients (settling time, overshoot) can be described via root location constraints in the complex plane using the parameters η, μ, and ξ. Note that the cases involving multiple roots of the characteristic equation are not considered here.

We will construct and verify all relevant surfaces in MATLAB. Due to their complexity, algebraic expressions will be handled using the *SymPy* library [22] of Python.

## 1. PROBLEM STATEMENT

Consider the characteristic equation of a fourth-order system:

$$a_0\lambda^4 + a_1\lambda^3 + a_2\lambda^2 + a_3\lambda + a_4 = 0. \qquad (1)$$

Equation (1) can be normalized by the transformation

$$\lambda = x \cdot \Omega_0 = x \cdot \sqrt[4]{\frac{a_4}{a_0}},$$

$$A = \frac{a_1}{\sqrt[4]{a_4 a_0^3}},\ B = \frac{a_2}{\sqrt[4]{a_4^2 a_0^2}},\ C = \frac{a_3}{\sqrt[4]{a_4^3 a_0}}.$$

The above scaling of the variable ensures the unit geometric mean root $\Omega_0$. The resulting normalized equation is

$$x^4 + Ax^3 + Bx^2 + Cx + 1 = 0. \qquad (2)$$

The Hurwitz stability criterion in the space of the parameters *A*, *B*, and *C* has the form [17]

$$A > 0, B > 0, C > 0,\ C(AB - C) - A^2 > 0; \qquad (3)$$

and the discriminant of equation (2) is expressed as follows:

$$\begin{aligned} D(A, B, C) = {} & 256 - 192AC - 128B^2 \\ & + 144BC^2 - 27C^4 + 144A^2B - 6A^2C^2 \\ & - 80AB^2C + 18ABC^3 + 16B^4 - 4B^3C^2 \\ & - 27A^4 + 18A^3BC - 4A^3C^3 - 4A^2B^3 + A^2B^2C^2. \end{aligned} \qquad (4)$$

Note that the surface of zero discriminant separates cases with different root locations and, by definition, indicates the presence of multiple roots. In real-world problems, multiple roots in a system are usually undesirable, and reaching the surface of zero discriminant means that the system parameters should be retuned.

For two real roots and a pair of complex conjugate roots, we should distinguish between cases with different root locations relative to the imaginary axis. In the Vyshnegradsky diagram, line *CD* serves to solve a similar task. For a fourth-order equation, the corresponding surface will be denoted by $G(A, B, C) = 0$. Hereinafter, we will refer to the spatial diagram consisting of the stability boundary surfaces, $D(A, B, C) =$ $= 0$, and $G(A, B, C) = 0$ as V-4 (Vyshnegradsky-4).

The use of a shifted equation to construct level lines for the stability degree was proposed in [3]. By introducing an equation with a right shift of η relative to (2), and using the Hurwitz criterion, one obtains equations of level lines for the stability degree. Similarly, level lines for ξ (the absolute value of the real part of the root with the largest distance to the imaginary axis) are obtained by shifting equation (2) to the right by ξ, followed by reflection relative to the imaginary axis. A shifted equation is also convenient to derive parametric-form equations of the curves dividing the Vyshnegradsky diagram into typical regions. Level lines for the oscillatory index are obtained using the relations derived from Viète's theorem for the normalized equation (2) with a pair of complex roots.

The shifted equation obtained by substituting $x = z - \eta$ is

$$z^4 + A_1z^3 + A_2z^2 + A_3z + A_4 = 0, \qquad (5)$$

where

$$A_1 = -4\eta + A,\ A_2 = 6\eta^2 - 3A\eta + B,$$
$$A_3 = -4\eta^3 + 3A\eta^2 - B\eta + C,$$
$$A_4 = \eta^4 - A\eta^3 + B\eta^2 - C\eta + 1. \qquad (6)$$

## 2. THE PARAMETERIZATION OF THE SURFACE *D*(*A*, *B*, *C*) = 0

The practical applicability of the cumbersome expression (4) is questionable, so we consider an alternative approach. The surface of zero discriminant $D(A, B, C) = 0$ corresponds to the presence of multiple roots of equation (2). Shifting the equation does not affect the relative position of the roots; therefore, $D(A, B, C) = 0$ if equation (5) has multiple roots. Clearly, the cases $A_3 = 0$ and $A_4 = 0$ correspond to a double zero root in equation (5):

$$z^4 + A_1z^3 + A_2z^2 = z^2(z^2 + A_1z + A_2) = 0.$$

Now, we write the conditions $A_3 = 0$ and $A_4 = 0$ in terms of $A$, $B$, C, and η:

$$\begin{cases} -4\eta^3 + 3A\eta^2 - B\eta + C = 0 \\ \eta^4 - A\eta^3 + B\eta^2 - C\eta + 1 = 0. \end{cases}$$

Elementary transformations yield

$$\begin{cases} A = \dfrac{1}{2}\left(\dfrac{B}{\eta} + 3\eta - \dfrac{1}{\eta^3}\right) \\ C = \dfrac{1}{2}\left(B\eta + \dfrac{3}{\eta} - \eta^3\right). \end{cases} \tag{7}$$

Actually, system (7) represents a parametric form of the surface $D(A, B, C) = 0$, where the coordinate $B$ itself is a parameter. This form is very convenient for constructing cross-sections by the planes $B = \text{const}$.

Note that the surface $D(A, B, C) = 0$ is symmetric with respect to the plane $A = C$. In equations (6), this symmetry is expressed as $A(B, \eta) = C(B, \frac{1}{\eta})$. The symmetric property can be utilized to simplify the construction procedure: first, one constructs a branch of the surface for $\eta \in [1, \eta_{\max}]$ and then reflects it symmetrically with respect to the plane $A = C$.

System (7) can be transformed in other ways as well, which is convenient for constructing cross-sections by other planes, e.g.,

$$\begin{cases} B = -3\eta^2 + 2A\eta + \dfrac{1}{\eta^2} \\ C = -2\eta^3 + A\eta^2 + \dfrac{2}{\eta}. \end{cases} \tag{8}$$

We emphasize that if $\eta = \text{const}$, the solutions of systems (7) and (8) will be straight lines (as the intersection of two planes). In other words, the surface of zero discriminant is formed by the spatial motion of a straight line.

## 3. THE PARAMETERIZATION OF THE SURFACE *G*(*A*, *B*, *C*) = 0

Let

$$x_1 = \alpha + i\beta, \qquad x_2 = \alpha - i\beta, \qquad x_3 = \gamma, \qquad x_4 = \delta$$

be the roots of equation (2). Since $\alpha = \delta$ and the two roots are complex conjugates, the fourth-order equation can be written as

$$((x-\alpha)^2 + \beta^2)(x-\alpha)(x-\gamma) = 0 .$$

After expanding the parentheses and collecting the coefficients at the powers of $x$, we compare the coefficients of the resulting expression with equation (2) to get the following nonlinear system of four equations:

$$\begin{cases} A = -3\alpha - \gamma \\ B = 3\alpha^2 + \beta^2 + 3\alpha\gamma \\ C = -\alpha^3 - 3\alpha^2\gamma - \alpha\beta^2 - \gamma\beta^2 \\ 1 = \alpha\gamma(\alpha^2 + \beta^2). \end{cases} \tag{9}$$

Clearly, the last equation of (9) can be used to reduce the number of variables:

$$\begin{cases} A = -3\alpha - \gamma \\ B = 2\alpha^2 + 3\alpha\gamma + \dfrac{1}{\alpha\gamma} \\ C = -\dfrac{\alpha + \gamma}{\alpha\gamma} - 2\alpha^2\gamma. \end{cases} \tag{10}$$

System (10) is a parameterization of the surface $G(A, B, C) = 0$. Constructing the surface with (10) in MATLAB requires thorough tuning to obtain a high-quality result. The first equation of this system can be used to eliminate the variable α or γ. Also, a different approach to parameterization should be tried here. We show that the cases $A_1A_2 - A_3 = 0$ and $A_4 = 0$ correspond to the presence of a zero and a pair of pure imaginary roots of the shifted equation (5):

$$z^4 + A_1z^3 + A_2z^2 + A_1A_2z = z\left(z^3 + A_1z^2 + A_2z + A_1A_2\right)$$
$$= z\left(z(z^2 + A_2) + A_1(z^2 + A_2)\right) = z\left((z^2 + A_2)(z + A_1)\right),$$
$$z_1 = 0, \quad z_{2,3} = \pm i\sqrt{A_2}, \quad z_4 = -A_1 .$$

Since equation (5) is shifted relative to (2), the conditions $A_1A_2 - A_3 = 0$ and $A_4 = 0$ correspond to the boundary between different arrangements of the roots of $G(A, B, C) = 0$. These conditions can be written as

$$\begin{cases} -20\eta^3 + 15A\eta^2 - (3A^2 - 2B)\eta + AB - C = 0 \\ \eta^4 - A\eta^3 + B\eta^2 - C\eta + 1 = 0. \end{cases} \tag{11}$$

Elementary transformations bring system (11) to the equivalent form

$$\begin{cases} B = -7\eta^2 + 3A\eta - \dfrac{1}{3\eta^2 - A\eta} \\ C = -6\eta^3 + 2A\eta^2 + \dfrac{2\eta - A}{3\eta^2 - A\eta}. \end{cases} \tag{12}$$

There are both first- and second-degree terms of the coefficient $A$ in the first equation of system (11).

Hence, other forms of the system with a single independent parameter η are difficult to write and impractical. Direct application of system (12) to construct the surface is difficult in cases of a vanishing denominator (when $A \approx 3\eta$). We plot the above surfaces of the spatial diagram *V*-4, as well as its cross-section by the plane *A* = const (Fig. 3).

## 4. LEVEL SURFACES FOR THE STABILITY DEGREE

In the diagram (Fig. 3), there are two regions where two complex conjugate roots have the smallest distance to the imaginary axis. For these regions, the shifted equation (5) reaches the oscillatory stability boundary, i.e., it has two roots in the left half-plane and a pair of pure imaginary roots. According to the Hurwitz criterion, this boundary is reached under the conditions

$$A_1A_2A_3 - A_1^2A_4 - A_3^2 = 0,\ A_1 > 0,\\ A_2 > 0,\ A_3 > 0,\ A_4 > 0. \tag{13}$$

Let us write the equality from (13) in terms of *A*, *B*, *C*, and η:

$$\begin{gathered} 64\eta^6 - 96A\eta^5 + 16(3A^2 + 2B)\eta^4 \\ - 8A(A^2 + 4B)\eta^3 + 4(2A^2B + AC + B^2 - 4)\eta^2 \\ - 2A(AC + B - 4)\eta + ABC - A^2 - C^2 = 0. \end{gathered} \tag{14}$$

In the other three regions of the *V*-4 diagram, the root of equation (5) closest to the imaginary axis is real, which corresponds to the aperiodic stability boundary of the shifted equation. This boundary is reached under the conditions

$$A_4 = 0,\ A_1 > 0,\ A_2 > 0,\ A_3 > 0,\\ A_1A_2A_3 - A_1^2A_4 - A_3^2 > 0. \tag{15}$$

After straightforward simplifications, the last inequality of (15) can be written as

$$A_1A_2 - A_3 > 0;$$

in terms of the parameters *A*, *B*, *C*, and η, this gives

$$-20\eta^3 + 15A\eta^2 - (3A^2 + 2B)\eta + AB - C > 0.$$

In the same terms, the first condition (equality) for the aperiodic stability boundary of the shifted equation takes the form

$$C = \eta^3 - A\eta^2 + B\eta + \frac{1}{\eta}. \tag{16}$$

For $\eta = \text{const}$, equation (16) defines a plane.

To construct level surfaces for the stability degree (Fig. 4), it is necessary to derive the surfaces (14) and (16) for the desired values of η that are bounded by the inequalities from (13) and (15), respectively.

The implicit definition of the surface (14) may be inconvenient for construction. We pass to its parametric definition using the change of parameters

$$k = \frac{A_3}{A_1}.$$

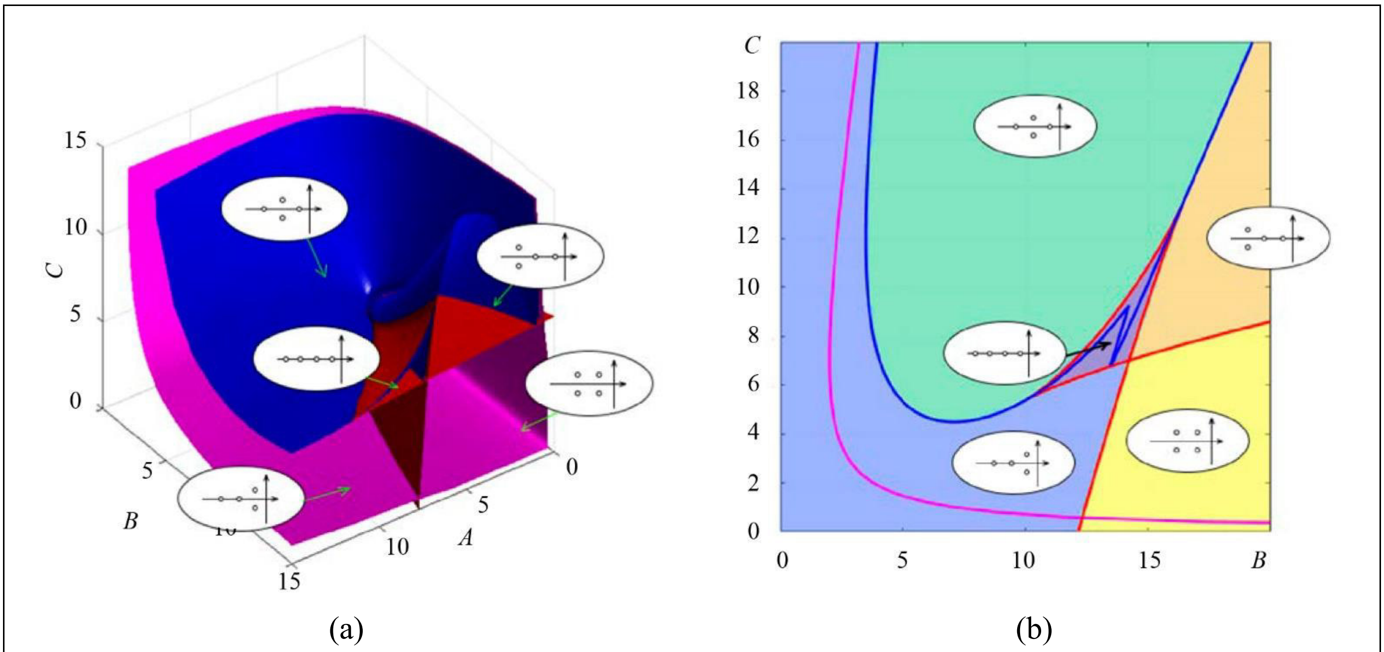


**Fig. 3. The *V*-4 diagram with typical root locations**: (a) the 3D diagram constructed using (3), (7) and (b) its cross-section by *A* = 7, constructed using (3), (8), and (12). The stability boundary is shown in lilac; *D*(*A*, *B*, *C*) = 0, in red; and *G*(*A*, *B*, *C*) = 0, in blue.

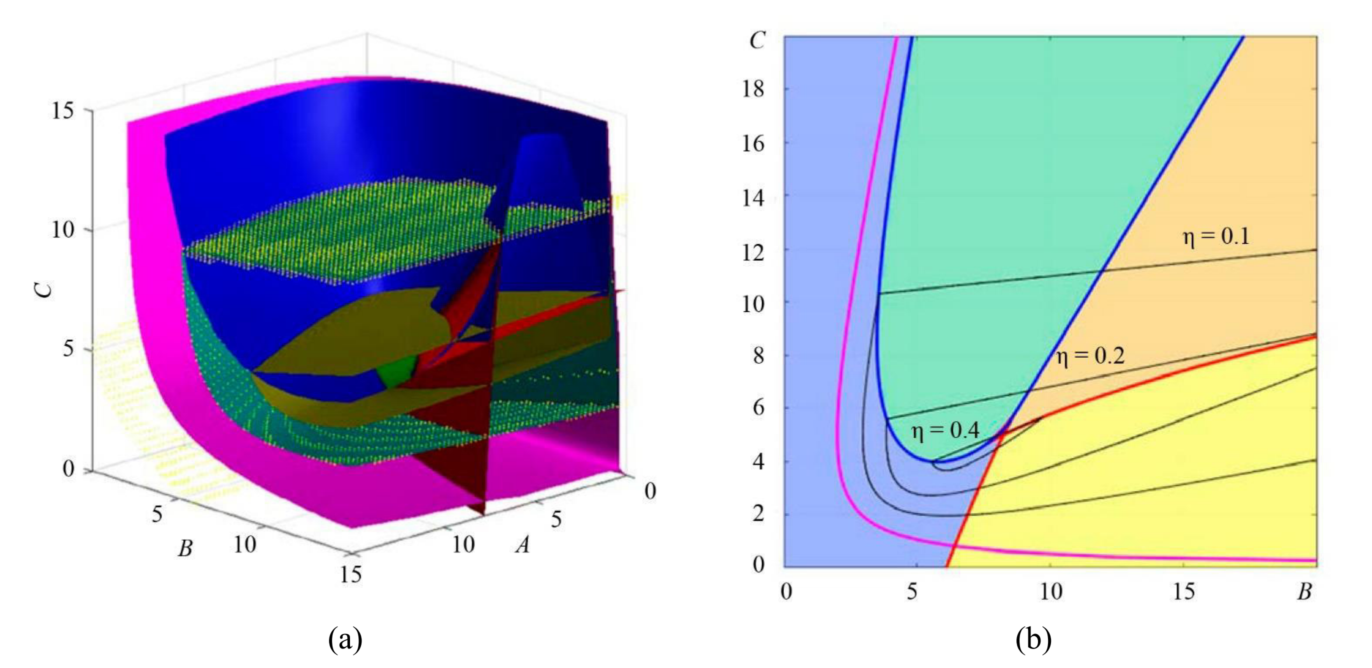


**Fig. 4. Level surfaces for the stability degree η:** (a) the 3D diagram with verification and (b) its cross-section by $A$ = 5.

Then the expression (12) takes the form

$$kA_1^2A_2 - A_1^2A_4 - k^2A_1^2 = A_1^2(kA_2 - A_4 - k^2) = 0.$$

In the region under consideration, $A_1 > 0$. Thus,

$$\begin{cases} A_3 - kA_1 = 0 \\ kA_2 - A_4 - k^2 = 0, \end{cases}$$

and trivial transformations of this system yield

$$\begin{cases} B = \dfrac{-3\eta^4 + 2A\eta^3 - 2k\eta^2 + 2Ak\eta + k^2 + 1}{\eta^2 + k} \\ C = \dfrac{-2\eta^5 + A\eta^4 - 4k\eta^3 + 2Ak\eta^2 - 2(k^2-1)\eta + Ak^2}{\eta^2 + k}. \end{cases} \quad (17)$$

System (17) is a convenient parameterization for a family of surfaces. The combined use of (8), (12), and (17) is well-suited for constructing cross-sections by planes $A$ = const.

Note that for $\eta = 0$, condition (14) coincides with the stability boundary condition for equation (2). The largest value of the stability degree $(\eta = 1)$ is achieved at the point $A$ = 4, $B$ = 6, $C$ = 4. (For verification, one should simply substitute the point into formulas (14) and (16).) This point corresponds to a Newtonian polynomial with the real root $x_{1,2,3,4} = -1$ of multiplicity 4. In other words, the region of real roots "begins" at this point.

Recall that the diagram shows the level surfaces for the normalized equation, and multiplication by the geometric mean root is required to pass to the stability degree of the original equation:

$$\eta_{\text{ori}} = \eta\Omega_0 = \eta \cdot \sqrt[4]{\frac{a_4}{a_0}}.$$

## 5. LEVEL SURFACES FOR THE MAXIMUM ABSOLUTE VALUE AMONG THE REAL PARTS OF ALL ROOTS

If the imaginary axis of the normalized equation (2) is shifted by ξ (the maximum absolute value among the real parts of all roots), the shifted equation will take the form

$$z^4 + A_1z^3 + A_2z^2 + A_3z + A_4 = 0 \quad (18)$$

where the coefficients $A_1$, $A_2$, $A_3$, and $A_4$ are given by formulas (6) with η replaced by ξ. The roots of equation (18), with the exception of those on the imaginary axis, are located in the right half-plane. By changing the variable $z$ to $-z$ in this equation, we obtain

$$z^4 - A_1z^3 + A_2z^2 - A_3z + A_4 = 0. \quad (19)$$

Here, all roots lying on the right side in equation (18) are located to the left of the imaginary axis.

If a real root of the shifted equation (19) is on the imaginary axis, and the other roots of the equation are in the left half-plane, then

$$\begin{aligned} &A_4 = 0,\ (-A_1) > 0,\ A_2 > 0, \\ &(-A_3) > 0,\ -A_1A_2 + A_3 > 0. \end{aligned} \quad (20)$$

In the case where a pair of imaginary roots of equation (19) lies on the imaginary axis, and the others lie in the left half-plane, we have

$$A_1A_2A_3 - A_1^2A_4 - A_3^2 = 0,$$
$$(-A_1) > 0,\ A_2 > 0,\ (-A_3) > 0,\ A_4 > 0. \quad (21)$$

Conditions (20) and (21) define level surfaces for $\xi$ in those regions where a real root and a pair of complex conjugate roots, respectively, has the largest distance to the imaginary axis.

The equalities in the expressions (20) and (21) coincide with equations (16) and (14), respectively. Thus, level surfaces for the maximum absolute values among the real parts of all roots (Fig. 5) are constructed by analogy with those for the stability degree; the sole distinction is that the surfaces are visualized in different regions.

To verify the above relationships for level surfaces for the stability degree and the maximum absolute value among the real parts of all roots, we plot on the diagrams (Figs. 4 and 5) the points corresponding to $\eta = 0.1 \pm 3\%$ and $\xi = 0.7 \pm 5\%$. These points were obtained by computing the roots of the fourth-order equation with the coefficients *A*, *B*, and *C* in MATLAB at each node of a uniform computational grid and determining the smallest ($\eta$) and largest ($\xi$) absolute values among the real parts of all roots at the nodes.

## 6. LEVEL SURFACES FOR THE OSCILLATORY INDEX

An oscillatory mode is possible only if the roots are complex conjugate. Let us express the fourth-order equation in terms of its roots, provided that two roots are complex conjugate:

$$((x-\alpha)^2 + \beta^2)(x-\gamma)(x-\delta) = 0\,. \quad (22)$$

After expanding the parentheses and collecting the coefficients at the powers of *x*, we compare the coefficients of the resulting expression with equation (2) to obtain the system

$$\begin{cases} A = -2\alpha - \gamma - \delta \\ B = \alpha^2 + \beta^2 + 2\alpha\gamma + 2\alpha\delta + \gamma\delta \\ C = -(\alpha^2+\beta^2)(\gamma+\delta) - 2\alpha\gamma\delta \\ 1 = \gamma\delta(\alpha^2+\beta^2). \end{cases}$$

By introducing the oscillation ratio $\mu = \dfrac{\beta}{\alpha}$ to eliminate the variable $\beta$, and also eliminating the variables $\gamma$

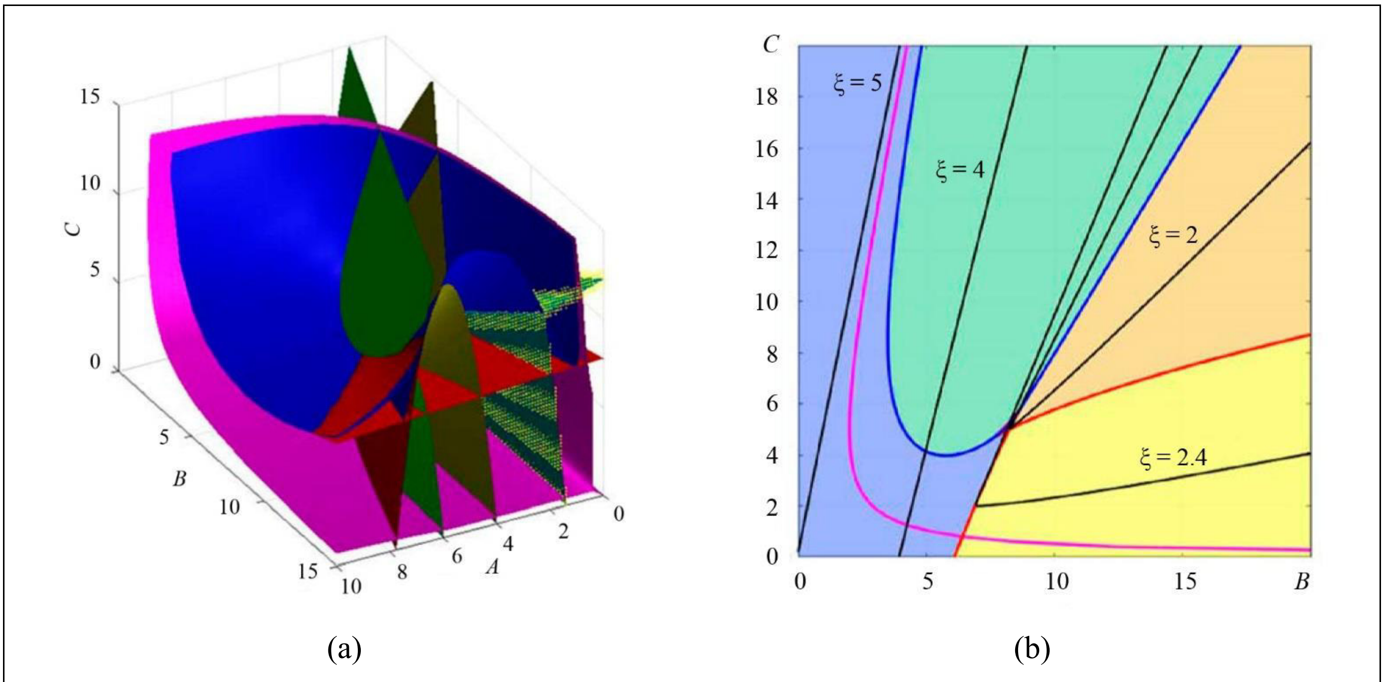


**Fig. 5. Level surfaces for the maximum absolute value $\xi$ among the real parts of all roots**: (a) the 3D diagram with verification (from left to right: $\xi$ = 3, $\xi$ = 2, and $\xi$ = 0.7) and (b) its cross-section by *A* = 5.

and δ, we arrive at the following parameterization of the desired surfaces:

$$\begin{cases} B = -2\alpha A - 3\alpha^2 + \alpha^2\mu^2 + \dfrac{1}{\alpha^2(1+\mu^2)} \\ C = \alpha^2(1+\mu^2)A + 2\alpha^3(1+\mu^2) - \dfrac{2}{\alpha(1+\mu^2)}. \end{cases} \quad (24)$$

Note that system (24) can be derived by using the equation

$$((x-\alpha)^2 + \beta^2)((x-\gamma)^2 + \delta^2)) = 0$$

instead of the expression (22). Clearly, without oscillations ($\mu = 0$), the system of equations (22) is equivalent to system (8), which defines the surface of zero discriminant. This can be rigorously established by the change of parameters $\alpha \to -\eta$. As the value of μ increases, the level surface for the oscillatory index gradually approaches the stability boundary; see Fig. 6.

This figure demonstrates several level surfaces for the oscillatory index, including the points corresponding to $\mu = 2 \pm 3\%$. These points were obtained by computing the roots of the fourth-order equation at each node of a uniform computational grid and determining the oscillatory index μ at the nodes directly from the roots.

According to the verification results, only the parts of the surfaces on one side of their self-intersection need to be plotted. Furthermore, the shape of the level surfaces for the oscillatory index suggests symmetry with respect to the plane *A* = *C*. Note that system (24) can also be written as

$$\begin{cases} A = \dfrac{\alpha^2(\mu^2-3) - B}{\alpha} + \dfrac{1}{2\alpha^3(1+\mu^2)} \\ C = \left(\alpha^3(1+\mu^2) - B\alpha\right)\dfrac{1+\mu^2}{2} - \dfrac{\mu^2-3}{2\alpha(1+\mu^2)}. \end{cases} \quad (25)$$

Therefore, $A(B, \mu, \alpha) = C\left(B, \mu, \dfrac{1}{\alpha(1+\mu^2)}\right)$, indicating the symmetry of the level surfaces $\mu = \text{const}$ with respect to the plane *A* = *C*. Due to the above symmetry, the self-intersection lines lie in this plane, which significantly simplifies the analysis. With $C = A$, the value of *A* can be expressed from the second equation of system (25). By substituting the resulting expression for *A* into the first equation of this system, we obtain the parametrically defined self-intersection curves

$$\begin{cases} A = C = -2\alpha - \dfrac{2}{\alpha(1+\mu^2)} \\ B = \alpha^2(1+\mu^2) + \dfrac{4\alpha^2+1}{\alpha^2(1+\mu^2)}. \end{cases} \quad (26)$$

The equations of the self-intersection lines being available, one can distinguish between surface points lying on opposite sides of these lines. When constructing level surfaces for the oscillatory index using formulas (24), the values of *A* and α are varied. It is pos-

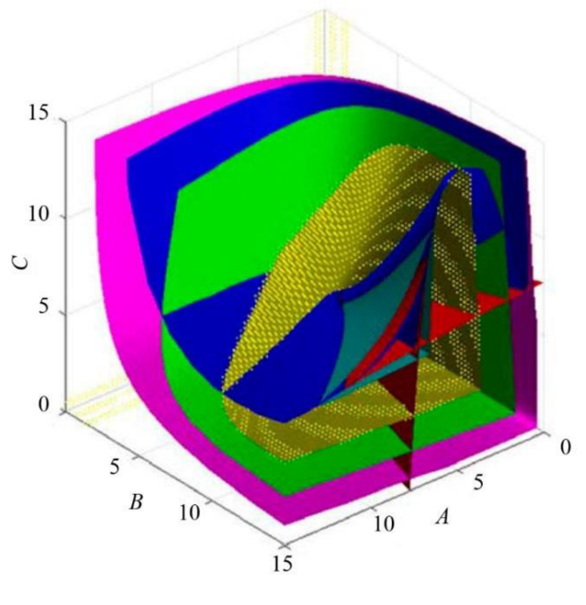


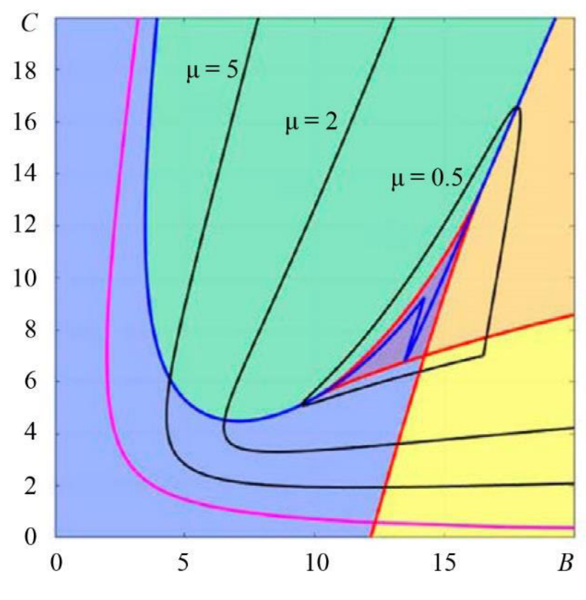


**Fig. 6. Level surfaces for the oscillatory index μ:** (a) the 3D diagram with verification and (b) its cross-section by *A* = 7.

sible to compute $A_{\text{line}}(\alpha, \mu)$ from the first equation of system (26) and plot only the points satisfying the condition $A > A_{\text{line}}$.

In addition, we emphasize that any level surface for the oscillatory index μ, like the surface of zero discriminant, is formed by the spatial motion of a straight line. And the symmetry of these level surfaces can be utilized to simplify the construction procedure by formulas (25): first, the surface part corresponding to $\alpha \in [\alpha_{\min}, -1]$ is plotted; then, it is reflected symmetrically with respect to the plane $A = C$.

Also, let us construct (Fig. 7) level surfaces for the oscillatory index in the parameters proposed in [8]:

$$\delta_1 = \frac{a_3^2}{a_2 a_4} = \frac{C^2}{B}, \quad \delta_2 = \frac{a_2^2}{a_1 a_3} = \frac{B^2}{AC}, \quad \delta_3 = \frac{a_1^2}{a_0 a_2} = \frac{A^2}{B}.$$

Obviously, these surfaces are easily approximated by level planes, providing sufficient and necessary conditions for a desired value of the oscillatory index [8].

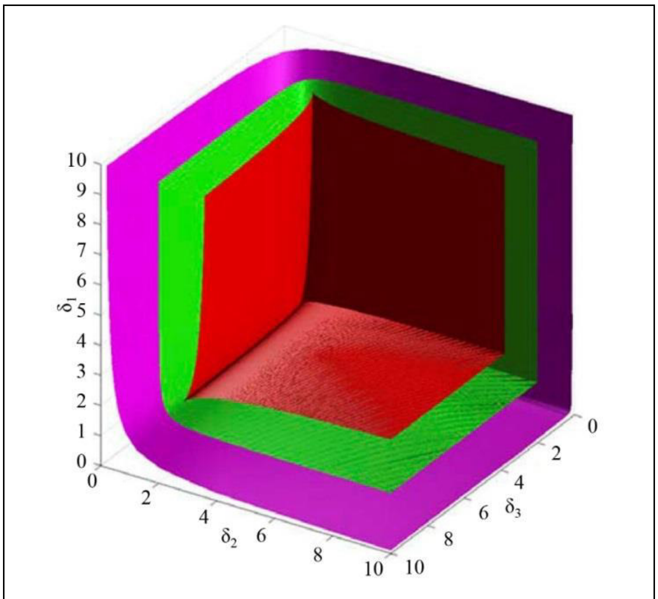


**Fig. 7. Level surfaces for the oscillatory index μ in the parameters $\delta_1$, $\delta_2$, and $\delta_3$**. The stability boundary (μ = ∞) is shown in lilac; μ = 0, in red; and μ = 1, in green.

Figure 8 shows the points corresponding to the standard Newton, Bessel, and Butterworth polynomials. Evidently, the latter two lie in the region corresponding to stable oscillatory processes, at a sufficient distance from the stability boundary.

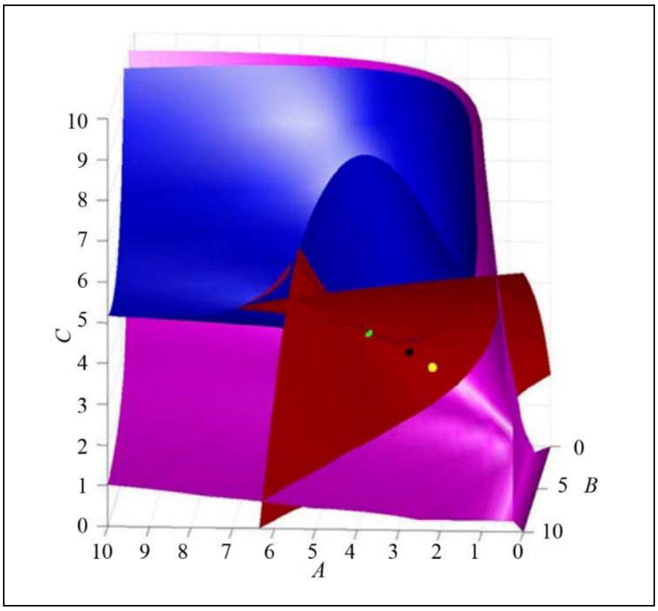


**Fig. 8. The *V*-4 diagram with points corresponding to standard polynomials:** Newton (green), Bessel (black), and Butterworth (yellow).

## CONCLUSIONS

In this paper, we have developed a complete analog of the Vyshnegradsky diagram for fourth-order characteristic equations. It has been implemented as a 3D diagram in the space of the parameters *A*, *B*, and *C* (the coefficients of the normalized equation (2)). The diagram highlights the main separating surfaces: the stability boundary, the surface of zero discriminant, and the boundary of various root locations to determine the dominant root type. Parametric expressions have been derived for families of level surfaces corresponding to specified system performance requirements: the stability degree (response speed), the oscillatory index (overshoot), and the absolute value of the real part of the root with the largest distance to the imaginary axis. An additional advantage is the parametric form of these surfaces, which simplifies their computation and visualization compared to implicit forms. Furthermore, all level surfaces can be defined either explicitly or in a manner convenient for constructing cross-sections. Based on such cross-sections, a user-friendly graphical interface can be created to view the transients and select appropriate normalized coefficients, as was done, e.g., in [4]. All level surfaces have been verified, and an example of their visualization in MATLAB has been provided.

The developed diagram is a tool for preliminary design. Also, it can be applied when creating a controlled object (plant). Subsequently, coefficients can be selected from the diagram under certain constraints of interest. For example, if the coefficients of the original characteristic equation actually depend on two parameters, then a surface can be constructed on the 3D diagram to select the coefficients. The points corresponding to Kharitonov polynomials can be plotted on the diagram if it is necessary to analyze the robust stability of the system or assess the spread of its performance indices. A most reasonable approach is to use the diagram in conjunction with software that simulates transients. Such a program complex can be easily implemented, e.g., using MATLAB.

## REFERENCES


1. Nesenchuk, A.A. and Opeiko, O.F., Synthesis of a Boiler Steam Pressure Robust Control System Using the Interval Systems Family Extended Root Locus, *DEStech Transactions on Engineering and Technology Research*, 2018, no. 13, pp. 434–439.
2. Patil, M.D., Vyawahare, V.A., and Bhole, M.K., A New and Simple Method to Construct Root Locus of General Fractional-Order Systems, *ISA Transactions*, 2014, vol. 53, no. 2, pp. 380–390.
3. Voronov, A.A., Titov, V.K., and Novogranov, B.N., *Osnovy teorii avtomaticheskogo regulirovaniya i upravleniya* (Foundations of the Theory of Automatic Regulation and Control), Moscow: Vysshaya Shkola, 1977. (In Russian.)
4. Kiselev, O.N. and Polyak, B.T., Design of Low-Order Controllers by the $H_\infty$ and Maximal-Robustness Performance Indices, *Autom. Remote Control*, 1999, vol. 60, no. 3, pp. 393–402.
5. Shcherbakov, P.S., Fixed Order Controller Design Subject to Engineering Specifications, *Automation and Remote Control*, 2010, vol. 71, no. 6, pp. 1217–1229.
6. Nesterov, A.V. and Nesterov, S.V., Vyshnegradsky's Diagram in MATLAB System, *Scientific Works of the Kuban State Technological University*, 2016, no. 13, pp. 88–99. (In Russian.)
7. Syrchina, A.S. and Kuleshov, A.V., Optimization of the Synthesis Method of the Indicator Gyrostabilizer Controller Using the Vyshnegradskii Criterion, *Izvestiya Tula State University. Technical Sciences*, 2023, no. 10, pp. 96–109. (In Russian.)
8. Petrov, B.N., Sokolov, N.I., Lipatov, A.V., et al., *Sistemy avtomaticheskogo upravleniya ob"ektami s peremennymi parametrami: Inzhenernye metody analiza i sinteza* (Automatic Control Systems for Variable Parameter Objects. Engineering Analysis and Design Methods), Moscow: Mashinostroenie, 1986. (In Russian.)
9. Baydoun, I., Analytical Formula for the Roots of the General Complex Quartic Polynomial, *hal-04693785*, 2024. URL: https://hal.science/hal-04693785v1 (Accessed November 10, 2025.)
10. Prodanov, E.M., Classification of the Real Roots of the Quartic Equation and Their Pythagorean Tunes, *International Journal of Applied and Computational Mathematics*, 2021, vol. 7, no. 4, art. no. 218.
11. Chávez-Pichardo, M., Martinez-Cruz, M.A., Trejo-Martínez, A., et al., A Complete Review of the General Quartic Equation with Real Coefficients and Multiple Roots, *Mathematics*, 2022, vol. 10, no. 14, art. no. 2377.
12. Polyak, B.T., Khlebnikov, M.V., and Shcherbakov, P.S., *Upravlenie lineinymi sistemami pri vneshnikh vozmushcheniyakh: Tekhnika lineinykh matrichnykh neravenstv* (Control of Linear Systems under Exogenous Disturbances: the Technique of Linear Matrix Inequalities), Moscow: LENAND, 2014. (In Russian.)
13. Zubov, N.E., Vorob'eva, E.A., Mikrin, E.A., et al., Synthesis of Stabilizing Spacecraft Control Based on Generalized Ackermann's Formula, *J. Comput. Syst. Sci. Int.*, 2011, vol. 50, no. 1, pp. 93–103.
14. Lapin, A.V. and Zubov, N.E., Simplifying the Formulas of Static Output Pole Placement for Fourth-Order Linear Time-Invariant Control Systems with Two Inputs and Two Outputs at Unequal Controllability and Observability Indices, *Differential Equations and Control Processes*, 2025, no. 3, pp. 1–11.
15. Moschytz, G.S. and Horn, P., *Active Filter Design Handbook: For Use with Programmable Pocket Calculators and Minicomputers*, Chichester: John Wiley & Sons, 1981.
16. Voronoi, V.V., A Polynomial Method for Calculating Multichannel Low-Order Controllers, *Extended Abstract of Cand. Sci. (Eng.) Dissertation*, Novosibirsk, 2013, p. 23. (In Russian.)
17. Sorokvashin, A.V., Kedrovskih, G.A., and Tatarinova, A.S., Constructing a Position Domain of the Fourth Order Polynomials with the Active Coefficient Roots, *Politechnical Student Journal of BMSTU*, 2025, no. 1 (96), pp. 1–17. (In Russian.)
18. Vasil'ev, V.A., *Geometriya diskriminanta* (The Geometry of the Discriminant), Moscow: Moscow Center for Continuous Mathematical Education, 2017. (In Russian.)
19. Rees, E.L., Graphical Discussion of the Roots of a Quartic Equation, *The American Mathematical Monthly*, 1922, vol. 29, no. 2, pp. 51–55.
20. Hong, H. and Yang, J., Parametric "Non-nested" Discriminants for Multiplicities of Univariate Polynomials, *Science China Mathematics*, 2024, vol. 67, pp. 1911–1932.
21. Mirer, S.A. and Prilepskii, I.V., Optimal Parameters of a Gravitational Satellite-Stabilizer System, *Preprints of the Keldysh Institute of Applied Mathematics*, 2008, no. 048, 28 p. (In Russian.)
22. SymPy. URL: https://www.sympy.org/ (Accessed November 10, 2025.)


*This paper was recommended for publication by M.V. Khlebnikov, a member of the Editorial Board.*

*Received December 29, 2025,*
*and revised March 26, 2026.*
*Accepted April 9, 2026.*

**Author information**
**Sorokvashin, Aleksandr Vladimirovich.** Student, Bauman Moscow State Technical University, Moscow, Russia
✉ sorokvashinav@student.bmstu.ru
ORCID iD: https://orcid.org/0009-0006-8979-0791

**Ignatov, Aleksandr Ivanovich.** Dr. Sci. (Eng.), Bauman Moscow State Technical University, Moscow, Russia
✉ ignatov@bmstu.ru
ORCID iD: https://orcid.org/0000-0001-6556-4585

**Cite this paper**
Sorokvashin, A.V. and Ignatov, A.I., Parametric Analysis of Root Location for a Fourth-Order Characteristic Equation. *Control Sciences* **4**, 24–34 (2026).



Translated into English by *Alexander Yu. Mazurov*,
Cand. Sci. (Phys.–Math.),
Trapeznikov Institute of Control Sciences,
Russian Academy of Sciences, Moscow, Russia
✉ alexander.mazurov08@gmail.com